Geol. Mag. **155** (*8*), *2018, pp. 1793–1810.*
doi:10.1017/S0016756817000735

Late Triassic ecosystem variations inferred by palynological records from Hechuan, southern Sichuan Basin, China

LIQIN LI*, YONGDONG WANG*†, VIVI VAJDA‡ & ZHAOSHENG LIU*

*State Key Laboratory of Palaeobiology and Stratigraphy, Nanjing Institute of Geology and Palaeontology, Chinese Academy of Sciences, Nanjing 210008, China
‡Swedish Museum of Natural History, Frescativägen 40, Stockholm 114 18, Sweden

(*Received* 28 January 2017; *accepted* 8 August 2017; *first published online* 26 September 2017)

Abstract – The Late Triassic deposits of the Sichuan Basin, southwestern China are significant for hosting abundant and diverse fossil assemblages including plants (containing spores and pollen), bivalves and insects. However, the Late Triassic palaeoecological variations are still poorly documented in this region. Here we present results from a palynological study from the Upper Triassic Xujiahe Formation in Hechuan of Chongqing, southern Sichuan Basin. The palynological analysis revealed a well-preserved terrestrial palynoflora of high diversity, comprising 184 species in 75 genera of spores and pollen. Three palynological assemblages were recognized, reflecting terrestrial successions throughout the entire interval with significant changes in the vegetation. Cycads/bennettites/ginkgophytes and conifers show an increasing trend into younger deposits, while ferns and lycopsids decrease in relative abundance. The Late Triassic vegetation underwent changes from lowland fern forest to a mixed forest with more canopy trees. We applied the Spore-pollen Morphological Group (SMG) method and Sporomorph EcoGroup (SEG) model to interpret the palaeoclimate features. The results reveal that the lower part of the Xujiahe Formation was deposited under relatively warm and humid conditions with an overall cooling and drying trend from latest Norian to Rhaetian time, accompanied by a general decrease of ferns and simultaneous increase of gymnosperms, and a decline in diversity of miospores. This study presents data on variations within the terrestrial ecosystem prior to the end-Triassic extinction event in the Sichuan Basin, and therefore provides important information for understanding the changes in the vegetation preceding the end-Triassic event.

Keywords: End-Triassic event, palynology, mass extinction, Sporomorph EcoGroup, climate change

1. Introduction

The end-Triassic mass extinction (201.36 ± 0.17 Ma; Schoene *et al*. 2010; Wotzlaw *et al*. 2014) is considered as one of the five largest Phanerozoic extinction events (Raup & Sepkoski, 1982; Sepkoski, 1996; Hesselbo, McRoberts & Pálfy, 2007), and massive biotic crises occurred in both the marine and terrestrial realms (Colbert, 1958; Pálfy *et al*. 2000; Hallam, 2002; Hesselbo *et al*. 2002; Olsen *et al*. 2002; Akikuni *et al*. 2010). In the ocean, the conodont animal became extinct and corals and molluscs such as bivalves and ammonites were seriously affected (Hallam, 1990, 2002; Tanner, Lucas & Chapman, 2004; Lucas & Tanner, 2007, 2008; Lathuilière & Marchal, 2009); on land, amphibians and reptiles suffered major losses (Colbert, 1958; Olsen, Shubin & Anders, 1987; Milner, 1989; Benton, 1991; Tanner, Lucas & Chapman, 2004; Lucas & Tanner, 2008). Within plant ecosystems, a major change took place with both reorganization and extinctions (McElwain *et al*. 2007; McElwain, Wagner & Hesselbo, 2009; Wang *et al*. 2010; Vajda & Bercovici, 2014; Sha *et al*. 2015; Lindström, 2016). Widespread magmatic activity of the Central Atlantic Magmatic Province (CAMP) has repeatedly been invoked to have triggered this catastrophic event (Marzoli *et al*. 1999, 2004; Wignall, 2001; Hesselbo *et al*. 2002; Hesselbo, McRoberts & Pálfy, 2007; van de Schootbrugge & Wignall, 2016). The most commonly accepted killing mechanism is rapid global warming driven by outgassing of CO_2 and release of methane (McElwain, Beerling & Woodward, 1999; Tanner, Lucas & Chapman, 2004; Bonis, Ruhl & Kürschner, 2010; Whiteside *et al*. 2010; Ruhl *et al*. 2011; Schaller, Wright & Kent, 2011; Steinthorsdottir, Jeram & McElwain, 2011; Schaller *et al*. 2012), and acidification of surface waters and terrestrial environments (van de Schootbrugge *et al*. 2009; Greene *et al*. 2012; Hönisch *et al*. 2012; Richoz *et al*. 2012; Callegaro *et al*. 2014; Ikeda *et al*. 2015; Bachan & Payne, 2016; van de Schootbrugge & Wignall, 2016).

In the palaeobotanical record, the end-Triassic event is typified by extinction of seed ferns including *Lepidopteris*, and the void was soon taken by dipteridacean ferns such as *Thaumatopteris* and a flora rich in conifers, ginkgoaleans and bennettites (McElwain *et al*.

†Author for correspondence: ydwang@nigpas.ac.cn

2007; Pott & McLoughlin, 2009, 2011; Vajda, Calner & Ahlberg, 2013; Mander, Kürschner & McElwain, 2013). This dramatic change is also expressed in the palynological record where Rhaetian and, in some places, early Hettangian successions host abnormal abundances of the enigmatic gymnosperm pollen *Ricciisporites tuberculatus* (Bonis, Ruhl & Kürschner, 2010; Mander, Kürschner & McElwain, 2013; Vajda, Calner & Ahlberg, 2013; Lindström, 2016). In the European record, a transitional zone dominated by fern spores has been identified (Ruckwied *et al*. 2008; Götz *et al*. 2009; Larsson, 2009; Ruckwied & Götz, 2009; van de Schootbrugge *et al*. 2009; Pieńkowski, Niedźwiedzki & Waksmundzka, 2012; Vajda, Calner & Ahlberg, 2013; Lindström, 2016). This interval in the Swedish record has been formalized as the 'Transitional Spore Spike Interval' (TSI) by Larsson (2009). This interval of pioneer vegetation is followed by the Hettangian floras characterized by high portions of *Classopollis* (Cheirolepidiaceae) recorded, for example from Sweden (Lund, 1977; Guy-Ohlson, 1981; Vajda, Calner & Ahlberg, 2013), Greenland (Pedersen & Lund, 1980; Mander, Kürschner & McElwain, 2013) and elsewhere.

With regards to the duration of the end-Triassic extinction, many workers argue that the extinction occurred over a prolonged interval marked by a series of discrete extinction events during Carnian–Rhaetian, rather than a single mass extinction at the end of the Rhaetian Age (Benton, 1986; Hallam, 2002; Tanner, Lucas & Chapman, 2004; Bambach, 2006; Lucas & Tanner, 2008, 2015; Wignall & van de Schootbrugge, 2016); studies on the Late Triassic ecosystem therefore form a very important role for better understanding the environmental changes prior to the end-Triassic extinction event.

In East Asia, the end-Triassic palaeobotanical and palynological records are somewhat scarce compared with Europe and North America. Two prime localities have so far been identified in China, both with well-exposed successions spanning the Triassic–Jurassic boundary, yielding diverse mega- and micro-floral records from terrestrial ecosystems. The regions include the Junggar Basin in the northwestern part of the country (Deng *et al*. 2010; Sha *et al*. 2011, 2015) and the Sichuan Basin in southwestern China (Wang *et al*. 2010). In particular, the Upper Triassic strata of the Xujiahe Formation are well developed in the Sichuan Basin, and contain diverse fossil plant assemblages (Ye *et al*. 1986; Huang & Lu, 1992; Huang, 1995; Wang *et al*. 2010). Recent magnetostratigraphic studies revealed that the age of the Xujiahe Formation ranges from latest Norian to Rhaetian (from 207.2 Ma to 201.3 Ma at Qilixia, Xuanhan, northeastern Sichuan Basin) (Li *et al*. 2017). Previous palynological studies on the Upper Triassic successions within the Sichuan Basin have contributed much to understanding the diversity and stratigraphy of the basin (Li, 1974; Cao & Huang, 1980; Liu, 1982; Bai *et al*. 1983; Zhang, 1984; Lu & Wang, 1987; Yuan, 1989; Huang, 1991; Shang & Li, 1992; Wang *et al*. 2008, 2010; Li & Wang, 2016). Recent efforts to decipher the regional responses of terrestrial plant communities prior to the end-Triassic event have been undertaken at several localities within the Sichuan Basin (Liu, Li & Wang, 2015*a*, *b*; Li *et al*. 2016). However, studies on the Late Triassic terrestrial palaeoenvironment based on palynology are still poorly documented in this region, thus our understanding on the Late Triassic ecosystem in the Sichuan basin therefore needs to be enhanced.

The present study documents a detailed palynological record from the Upper Triassic Xujiahe Formation of the Tanba section in the Hechuan region, southern Sichuan Basin (Fig. 1). Based on our palynological data, we aim to: (1) describe the Late Triassic vegetation in terms of abundance and diversity; and (2) decipher the Late Triassic climate variations in the studied area and place the results in a broader palaeogeographical context of the Late Triassic Period.

2. Geological setting

Located at the western margin of the South China block and the eastern margin of the Tibet Plateau, the Sichuan Basin is a large terrestrial petroliferous and coal-bearing basin, covering an area of 260 000 km^2 (Wang *et al*. 2010). It is bounded to the west by the Longmenshan orogenic belt, to the east by the Xuefengshan intercontinental tectonic deformation system, to the north by the Micangshan and Dabashan uplift belts, and to the south by the Emeishan–Liangshan fault-fold belt (Wang *et al*. 2010). Palaeozoic – early Mesozoic marine strata are well developed in the adjacent mountain areas, including Precambrian, Cambrian, Ordovician, Silurian, Carboniferous, Permian and Lower–Middle Triassic deposits. The Upper Triassic is dominated by terrestrial successions, mainly distributed in the eastern and northeastern margin of the basin. The remaining part of the basin is covered by massive Jurassic and Cretaceous red beds (Wang *et al*. 2010; Fig. 1).

Most importantly, the Upper Triassic strata represented by the Xujiahe Formation mainly consist of coal-bearing clastic rocks deposited in an inland lacustrine–fluvial–coal-swamp environment, varying over 400–650 m in thickness (Wang *et al*. 2010). The coal seams, which contain diverse plant remains (e.g. Xujiahe flora), play an important economic and scientific role in the Sichuan Basin (Wang *et al*. 2010).

The Xujiahe Formation is well exposed at the Tanba Section in the Hechuan region, southern Sichuan Basin (Fig. 1), administratively belonging to Chongqing City. The Xujiahe Formation overlies the Middle Triassic marine Leikoupo Formation and is, in turn, conformably overlain by the terrestrial Lower Jurassic Zhenzhuchong Formation (Fig. 2). At the Tanba section, an *c.* 500 m outcrop of the Xujiahe Formation is well exposed. The lithology mainly comprises sandstones, siltstones, mudstones and coal beds, yielding a diverse and rich fossil assemblages of plants and

https://doi.org/10.1017/S0016756817000735 Published online by Cambridge University Press

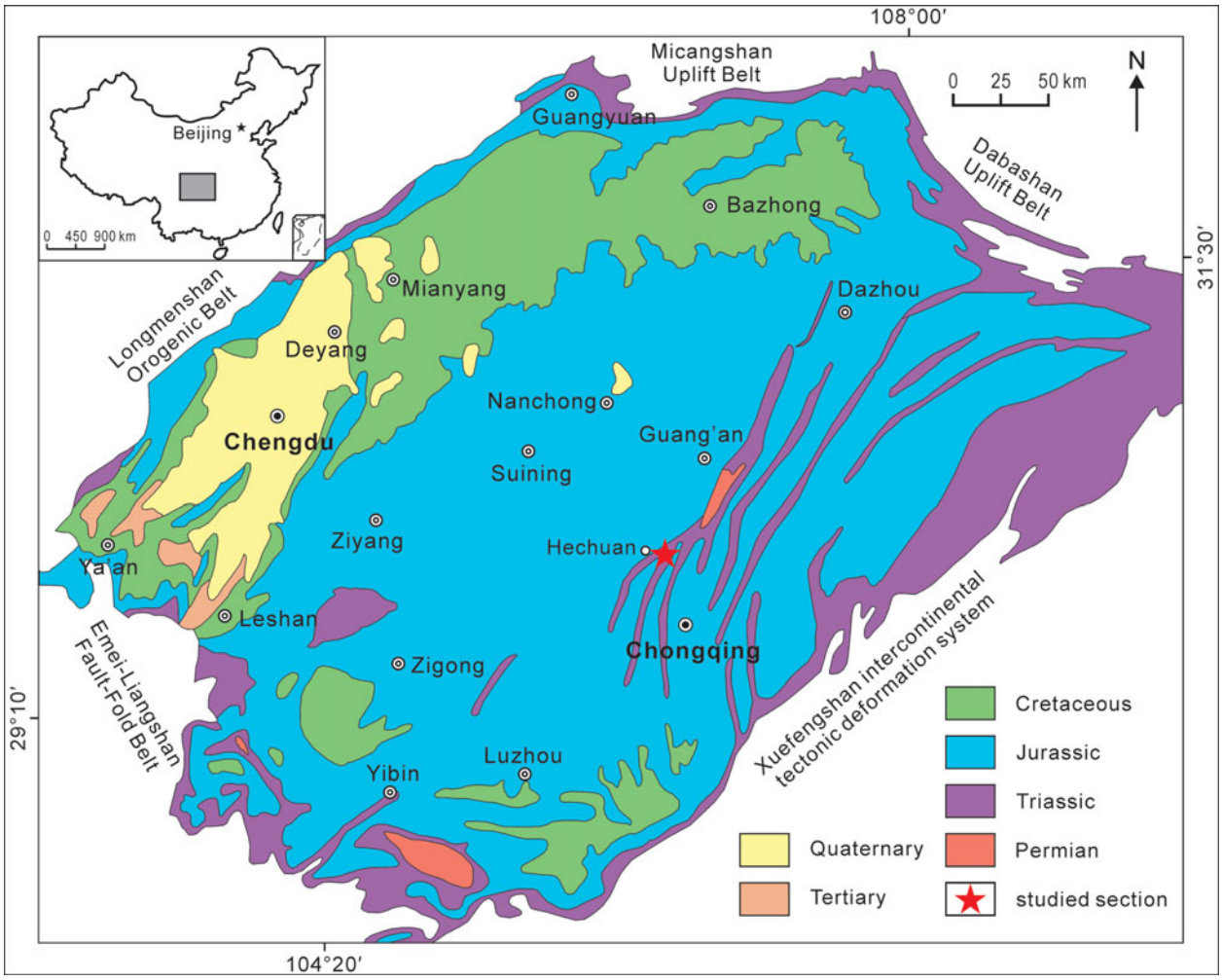

Figure 1. Simplified geological map of the Sichuan Basin showing the geological background and the location of the studied section (modified from Wang *et al*. 2010).

bivalves. The Xujiahe Formation is subdivided into six lithological members (I–VI), numbered in ascending order. Members I, III and V are mainly dominated by mudstones and thin coal beds, representing floodplain–lacustrine and coal swamp deposits, whereas members II, IV and VI mainly comprise sandstones, representing fluvial-delta deposits (Fu *et al*. 2010; Wang *et al*. 2010; Fig. 2).

3. Materials and methods

Thirty-three palynological samples were collected from the Upper Triassic Xujiahe Formation (from the members I–VI) across the Tanba section in the Hechuan region. Eighteen samples were productive and yielded well-preserved and rich miospores (spores and pollen). No productive samples were however recovered from Member II (Fig. 2). All the productive samples were collected from organic-rich mudstones, siltstone and coal, therefore minimizing the taphonomic bias.

For palynological preparation, approximately 30 g of sediment was treated with HCl and HF to remove carbonates and silicate minerals, respectively. The residue of each sample was then washed with distilled water until a neutral pH was reached. The residue was subsequently sieved through a 10 μm size mesh. Finally, the palynomorph-bearing residues were mounted on slides using glycerin jelly, and were sealed with paraffin wax. At least *c.* 250 sporomorphs were counted per sample. All samples were studied using an Olympus BX41 microscope. Photomicrographs were taken using a Zeiss Imager Z2 microscope and an AxioCam HRc imaging system. The SMG (Spore-pollen Morphological Group) method outlined by Visscher & Van der Zwan (1981) and the SEG (Sporomorph EcoGroup) model established by Abbink (1998) and Abbink, van Konijnenburg-van Cittert & Visscher (2004) were applied in this study to reconstruct the palaeoclimatic variations. All palynological slides are stored at the Nanjing Institute of Geology and Palaeontology, Chinese Academy of Sciences, Nanjing, China.

4. Palynology

The miospores of the Xujiahe Formation in the Hechuan Section of Chongqing City, southern Sichuan

https://doi.org/10.1017/S0016756817000735 Published online by Cambridge University Press

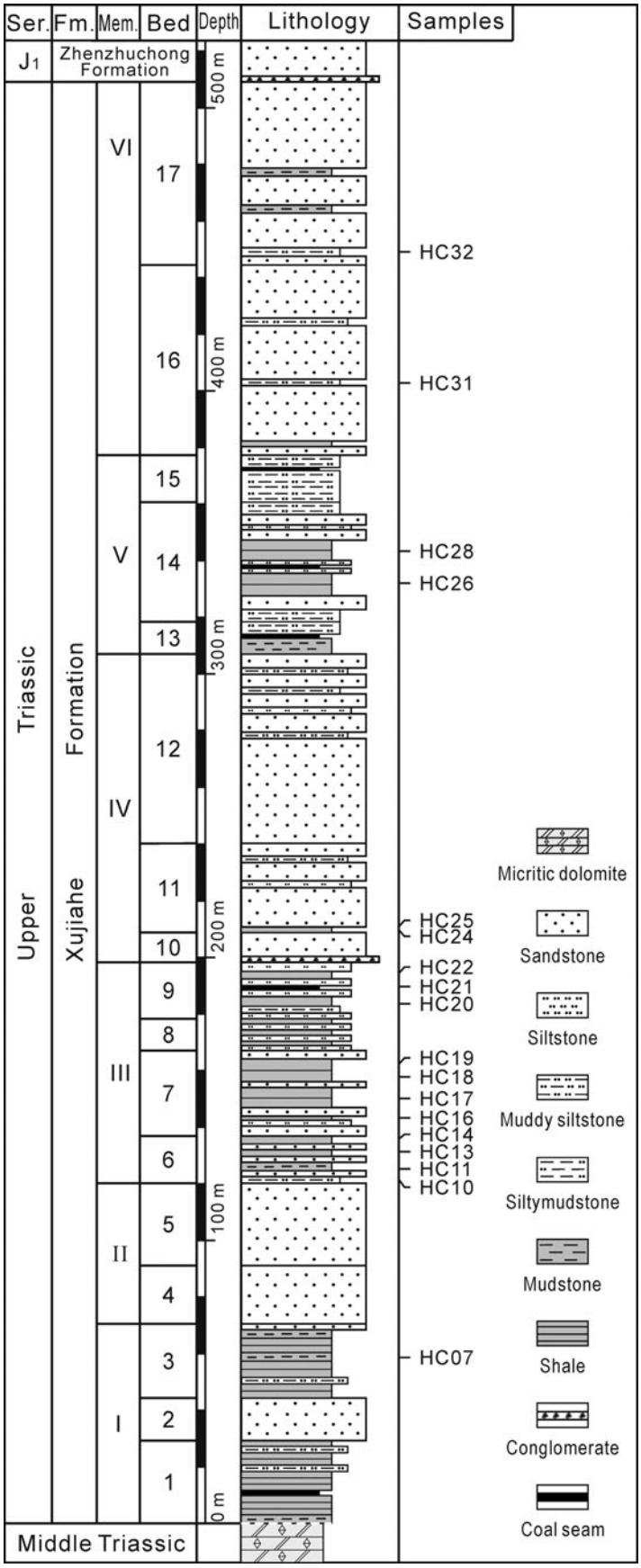

Figure 2. Stratigraphic column of the Tanba Section of the Xujiahe Formation, indicating the beds sampled for palynology.

https://doi.org/10.1017/S0016756817000735 Published online by Cambridge University Press

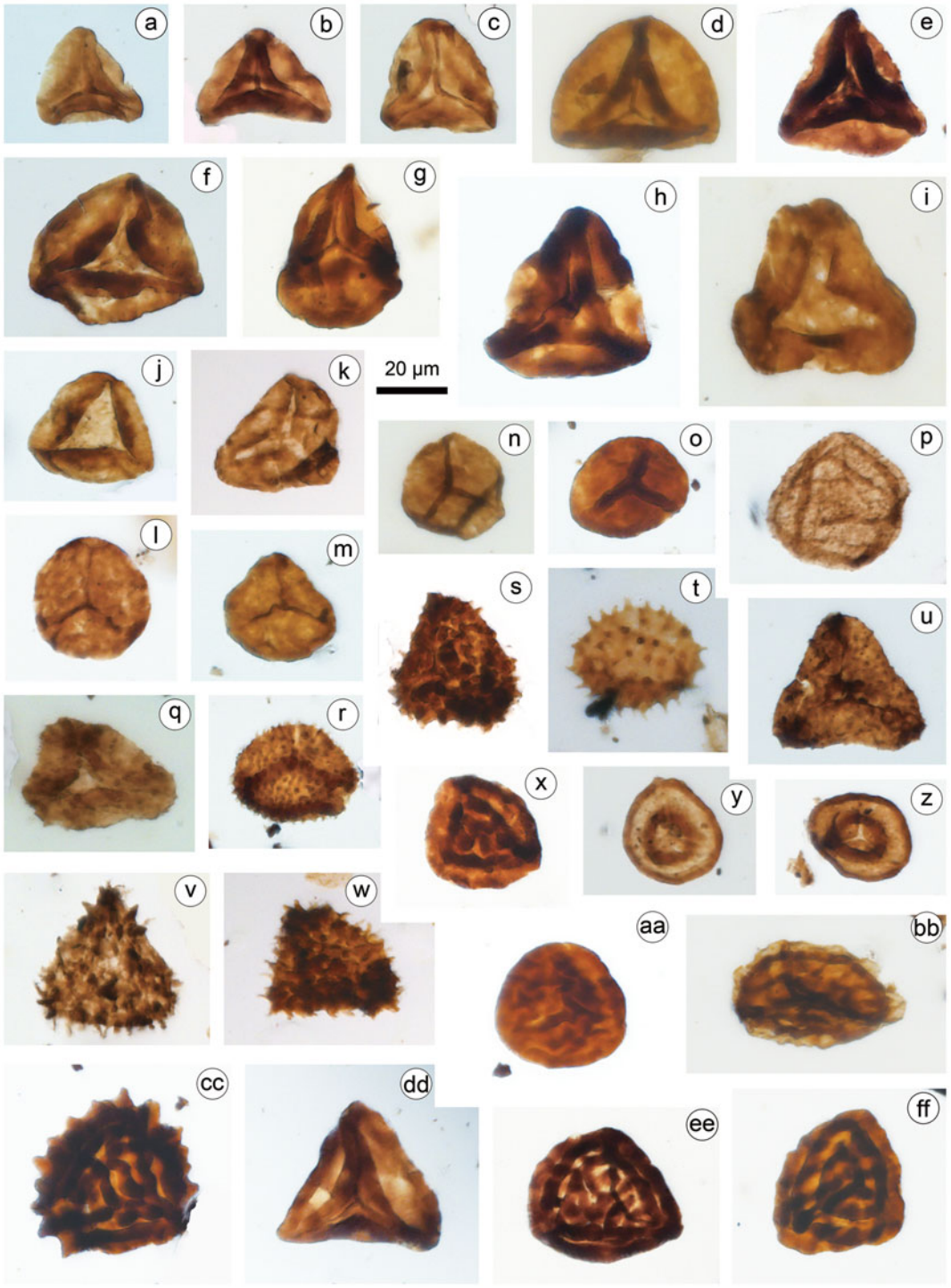

Figure 3. (Colour online) Representative spore taxa recovered from the Xujiahe Formation of the Hechuan region. Taxa names are followed by slide number. (a–c) *Dictyophyllidites harrisii*: (a, b) HC10-1; (c) HC11-3. (d) *Dictyophyllidites mortonii*, HC26-6. (e–h) *Concavisporites toralis*: (e) HC10-4; (f–h) HC9-1. (i) *Cyathidites australis*, HC28-2. (j, k) *Cyathidites minor*: (j) HC13-2; (k) HC18-4. (l) *Punctatisporites triassicus*, HC13-1. (m) *Leiotriletes adnatus*, HC13-2. (n) *Leiotriletes toroiformis*, HC26-1. (o) *Toroisporis* sp., HC10-6. (p) *Osmundacidites wellmanii*, HC13-1. (q) *Lunzisporites lunzensis*, HC30-2. (r, t) *Anapiculatisporites spiniger*: (r) HC11-6; (t) HC24-6. (s) *Lophotriletes sparsus*, HC18-2. (u) *Granulatisporites granulatus*, HC13-1. (v, w) *Acanthotriletes aculeatus*: (v) HC17-3; (w) HC18-4. (x, ee) *Asseretospora gyrata*, HC13-3. (y, z) *Annulispora folliculosa*: (y) HC11-2; (z) HC13-1. (aa) *Lycopodiacidites rudis*, HC11-4. (bb) *Lycopodiumsporites* sp., HC13-5. (cc) *Asseretospora curvata*, HC13-1. (dd) *Kyrtomisporis laevigatus*, HC10-2. (ff) *Asseretospora scanicus*, HC13-3.

Basin are diverse and well preserved, represented by 184 species of spores and pollen in 75 genera (see online Supplementary Table S1, available at http://journals.cambridge.org/geo). The representative miospores are illustrated in Figures 3–5. The palynoflora of the Xujiahe Formation from the Hechuan region has previously been assigned a Norian–Rhaetian age (Liu, Li & Wang, 2015*b*), which is

https://doi.org/10.1017/S0016756817000735 Published online by Cambridge University Press

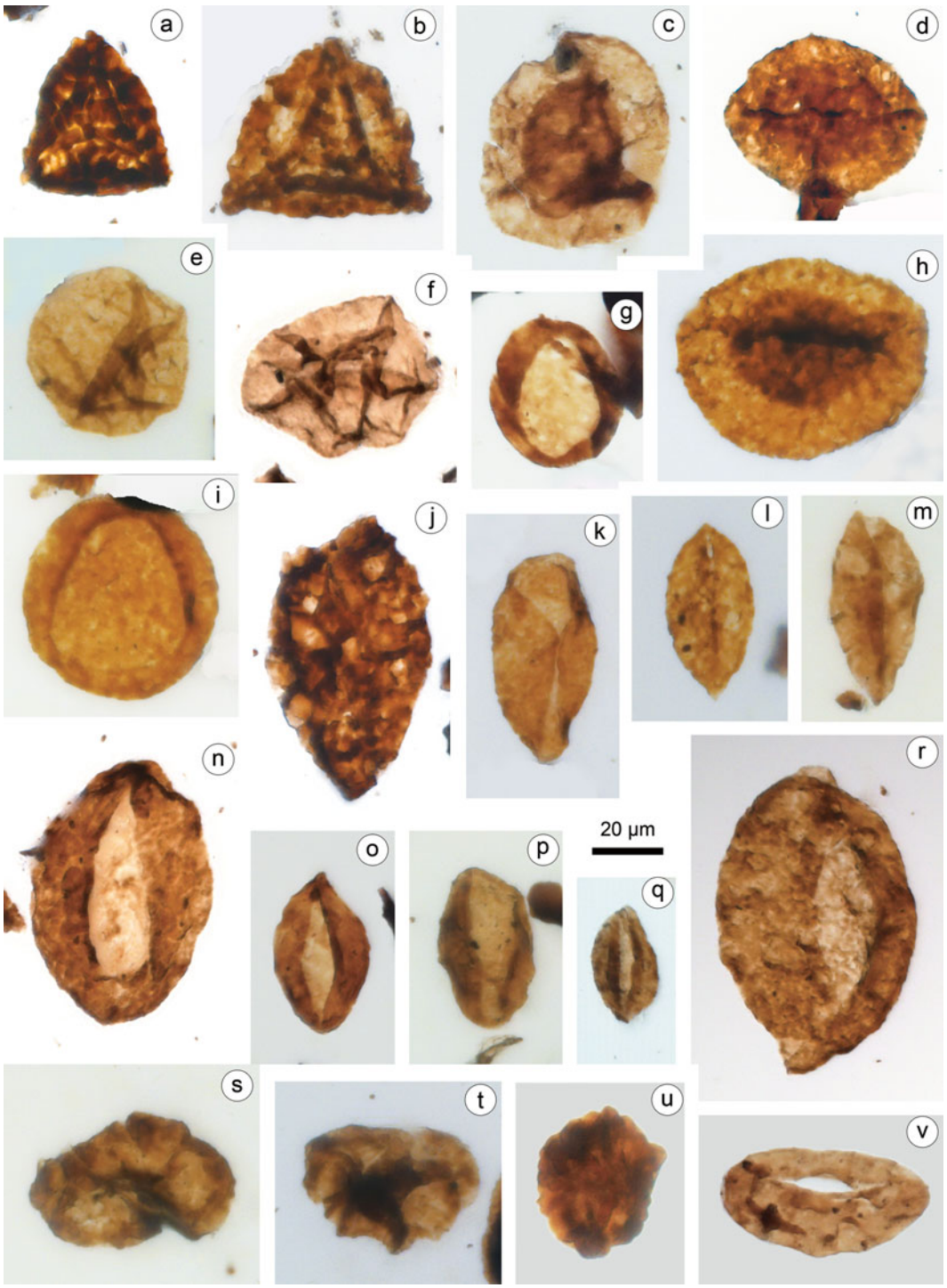

Figure 4. (Colour online) Representative miospore taxa recovered from the Xujiahe Formation of the Hechuan region. Taxa names are followed by slide number. (a, b) *Kyrtomisporis speciosus*: (a) HC17-4; (b) HC21-6. (c) *Kraeuselisporites punctatus*, HC11-1. (d, h) *Aratrisporites scabratus*: (d) HC13-6; (h) HC20-3. (e, f) *Araucariacites australis*: (e) HC26-5; (f) HC18-2. (g) *Chasmatosporites apertus*, HC11-1. (i) *Chasmatosporites hians*, HC32-5. (j) *Cycadopites reticulata*, HC7-3. (k) *Cycadopites pyriformis*, HC24-1. (l) *Cycadopites typicus*, HC20-1. (m) *Cycadopites deterius*, HC28-2. (n) *Chasmatosporites major*, HC18-2. (o, q) *Monosulcites minimus*: (o) HC11-2; (q) HC13-2. (p) *Monosulcites enormis*, HC31-5. (r) *Monosulcites fusiformis*, HC18-3. (s, t) *Classopollis minor*: (s) HC32-5; (t) HC25-1. (u) *Uvaesporites* sp., HC31-4. (v) *Ovalipollis ovalis*, HC11-4.

supported by a recent geomagnetic study (Li *et al.* 2017). Here we provide a more detailed vegetation reconstruction coupled with palaeoclimatic interpretations through the studied succession. For palaeoclimatic and palaeoecological purposes, the palynological assemblages were divided based on relative abundance. Three assemblages were recognized and the percentages of selected taxa are illustrated in Figure 6. The characteristic features for each assemblage are outlined below in ascending stratigraphic order. The percentages are expressed in whole numbers.

https://doi.org/10.1017/S0016756817000735 Published online by Cambridge University Press

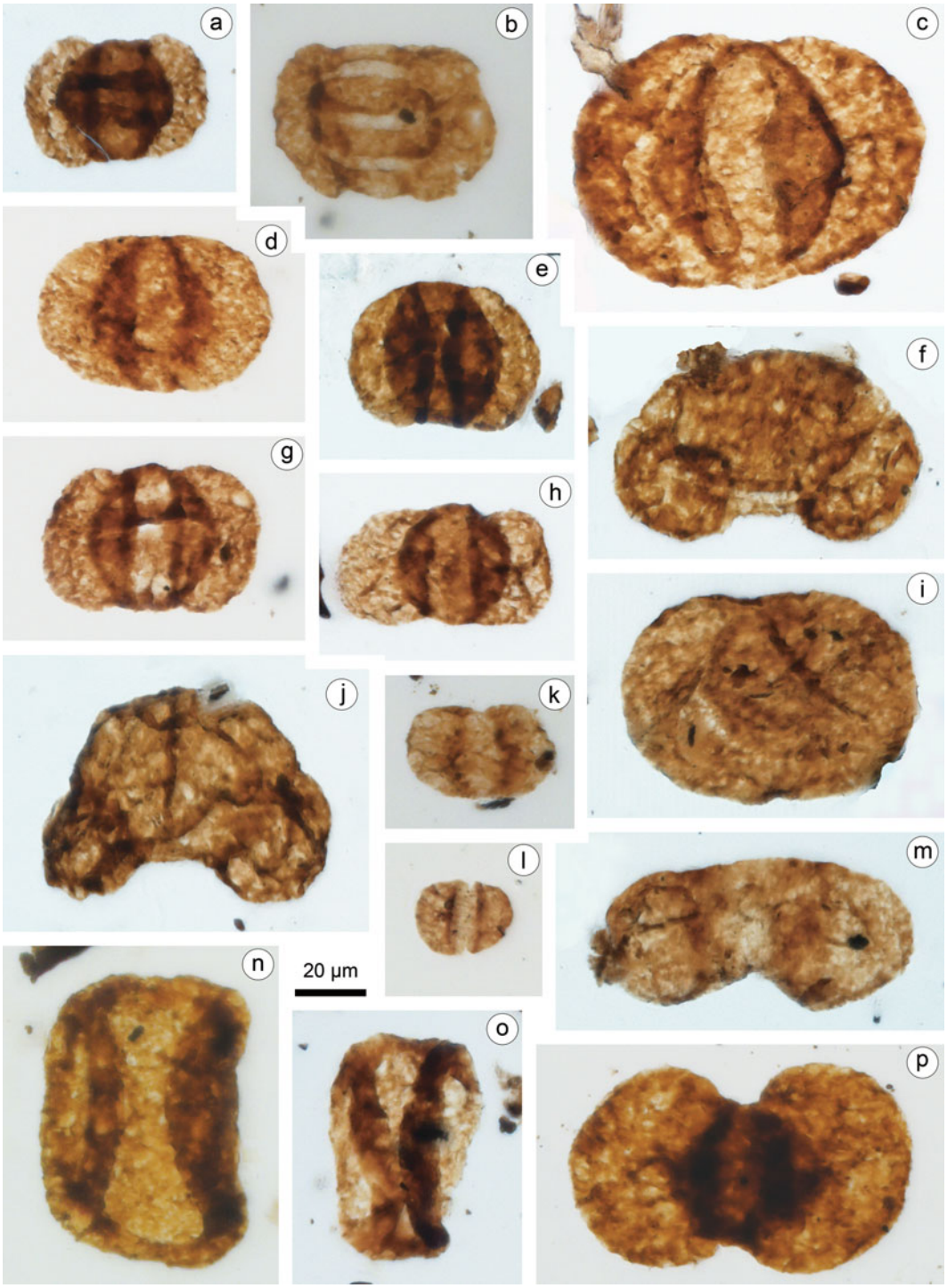

Figure 5. (Colour online) Representative pollen taxa recovered from the Xujiahe Formation of the Hechuan region. Taxa names are followed by slide number. (a) *Lueckisporites triassicus*, HC13-2. (b) *Taeniaesporites noviaulensis*, HC13-5. (c) *Alisporites australis*, HC13-1. (d) *Alisporites parvus*, HC13-1. (e) *Alisporites bilateralis*, HC13-2. (f) *Pinuspollenites divulgatus*, HC13-2. (g, h) *Pinuspollenites enodatus*, HC13-1. (i) *Paleoconiferus asaccatus*, HC13-2. (j) *Pinuspollenites alatipollenites*, HC13-2. (k, l) *Vitreisporites pallidus*: (k) HC13-4; (l) HC13-1. (m) *Podocarpidites multisimus*, HC13-2. (n, o) *Quadraeculina anellaeformis*: (n) HC21-1; (o) HC11-3. (p) *Platysaccus queenslandi*, HC13-4.

4.a. *Dictyophyllidites harrisii – Concavisporites toralis – Kyrtomisporis laevigatus – Aratrisporites fischeri* (DCKA) assemblage (samples HC07–HC10)

The DCKA assemblage is identified in Member I and within the base of Member III of the Xujiahe Formation (Fig. 6). It is characterized by a significant dominance of spores (average 77 %), highly dominated by trilete fern spores (mostly produced by ground ferns) represented mainly by *Concavisporites*/*Dictyophyllidites* (23 %), followed by *Leiotriletes* (8 %), *Kyrtomisporis* (7 %), *Granulatisporites* (6 %), *Cyathidites* (4.5 %) and *Toroisporis* (3 %). Other spore genera occurring in lower abundances (1–3 %) within

https://doi.org/10.1017/S0016756817000735 Published online by Cambridge University Press

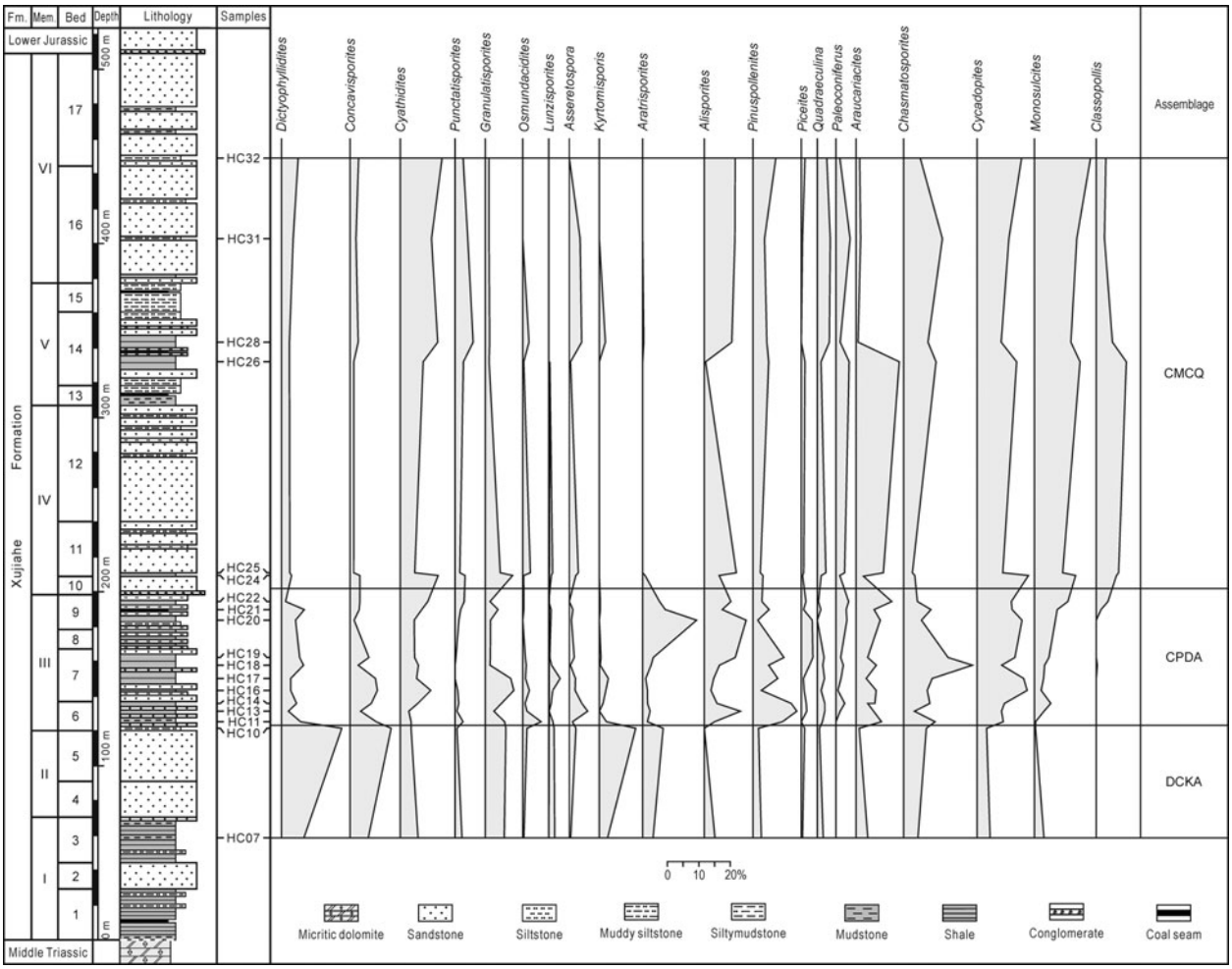

Figure 6. Abundance diagram of major spore-pollen genera and assemblages represented in the samples from the Xujiahe Formation in the Tanba Section of the Hechuan region.

this assemblage include *Uvaesporites*, *Klukisporites*, *Lunzisporites*, *Punctatisporites*, *Planisporites*, *Asseretospora*, *Sphagnumsporites*, *Anapiculatisporites* and *Kraeuselisporites*. Monolete spores comprise >5 % and are mainly represented by *Aratrisporites* produced by lycophytes (Fig. 6; Table 1).

In the DCKA assemblage, gymnosperm pollen grains reach an average of 24 % which are dominated by monocolpate pollen grains (average 11 %, including *Chasmatosporites*, *Cycadopites* and *Monosulcites*). Bisaccate conifer pollen grains reach average relative abundance of 6 % (including *Pinuspollenites*, *Protopinus*, *Piceites*, *Pseudopicea*, *Podocarpidites*, *Quadraeculina*, *Protoconiferus*, *Chordasporites* and *Taeniaesporites*). Bisaccate seed fern pollen (including *Alisporites* and *Vitreisporites*) are less abundant (*c.* 2 %) (Fig. 6).

4.b. *Cycadopites reticulata – Pinuspollenites divulgatus – Dictyophyllidites harrisii – Aratrisporites fischeri* (CPDA) assemblage (samples HC11–HC22)

The CPDA assemblage occurs in the upper part of Member III of the Xujiahe Formation (Fig. 6). It is characterized by the predominance of gymnosperm pollen grains (average relative abundance of 56 %) and a significantly lower portion of spores (44 %) compared to the other two assemblages.

Monocolpate pollen grains dominate (average of *c.* 26 %), represented by *Cycadopites* (11 %), *Chasmatosporites* (10 %) and *Monosulcites* (5 %). Bisaccate conifer pollen grains are the second-most abundant type (average 15 %), represented by *Pinuspollenites* (7 %), *Paleoconiferus* (2 %), *Piceites* (2 %), *Quadraeculina* (2 %) and *Pseudopicea* (1 %). Bisaccate seed fern pollen (including *Alisporites* and *Vitreisporites*) and *Araucariacites* increase in abundance (7 % and 6 %, respectively). *Classopollis* is rare (0.5 %), and shows a distinct increase in the uppermost part of this assemblage (Fig. 6).

Trilete spores are the dominant type among spores in the CPDA assemblage (average 39 %), marked mainly by *Concavisporites*/*Dictyophyllidites* (10 %), *Cyathidites* (6 %) and *Granulatisporites* (4 %). Other spore genera are common (1–3 %) in this assemblage such as *Asseretospora*, *Osmundacidites*, *Lophotriletes*, *Acanthotriletes*, *Conbaculatisporites*, *Cyclogranisporites*, *Punctatisporites* and *Kyrtomisporis*. Monolete spores are also common (5 %), and are mainly represented by *Aratrisporites* produced by lycophytes (4 %) (Fig. 6).

https://doi.org/10.1017/S0016756817000735 Published online by Cambridge University Press

Table 1. Botanical affinity and classification of the Sporomorph EcoGroup (SEGs) for dispersed miospores of the Xujiahe Formation in the Hechuan region, southern Sichuan Basin, China

Botanical affinity	Sporomorph genera	SEG	Ecological remarks
Horsetails	*Calamospora*	Lowland	Wetter, warmer
Ferns (Dipteridaceae/ Matoniaceae)	*Dictyophyllidites*, *Concavisporites*		
Ferns (Dipteridaceae)	*Kyrtomisporis*, *Apiculatisporis*, *Granulatisporites*		
Ferns (Osmundaceae)	*Punctatisporites*, *Todisporites*, *Osmundacidites*, *Conbaculatisporites*, *Baculatisporites*		
Ferns (Dicksoniaceae)	*Cibotiumspora*, *Converrucosisporites*		
Ferns (Cyatheaceae/ Dicksoniaceae)	*Cyathidites*		
Ferns (Pteridaceae)	*Asseretospora*		
Ferns (Marattiaceae)	*Angiopteridaspora*, *Toroisporis*, *Cyclogranisporites*, *Marattisporites*		
Ferns	*Leiotriletes*, *Lophotriletes*, *Lunzisporites*, *Planisporites*, *Tripartina*, *Brochotriletes*, *Klukisporites*, *Dictyotriletes*, *Foveotriletes*, *Reticulatisporites*, *Triquitrites*		
Cycads/bennettites	*Cycadopites, Monosulcites*	Lowland	Drier, warmer
Cycads	*Chasmatosporites*	Lowland	Drier, cooler
Ginkgophytes	*Monosulcites minimus*		
Conifers (Cheirolepidiaceae)	*Classopollis*	Lowland	Drier, warmer
Gymnosperms	*Tubermonocolpites*, *Verrumonocolpites*	Lowland	Drier, cooler
Conifers (Taxodiaceae)	*Inaperturopollenites*	Lowland	Wetter, cooler
Conifers (Pinaceae)	*Piceites*, *Pinuspollenites*	Upland	
Conifers (Podocarpaceae)	*Podocarpidites*, *Protopodocarpus*, *Quadraeculina*, *Taeniaesporites*, *Platysaccus*		
Conifers (Araucariaceae)	*Araucariacites*		
Conifers	*Protopinus*, *Pseudopinus*, *Pseudopicea*, *Protoconiferus*, *Paleoconiferus*		
Pinaceae/Cycads	*Ovalipollis*		
Gymnosperm	*Cordaitina*, *Lueckisporites*, *Chordasporites*		
Mosses	*Sphagnumsporites*, *Annulispora*, *Polycingulatisporites*	River	
Horsetails	*Retusotriletes*, *Laevigatosporites*		
Lycopsids	*Lycopodiumsporites*, *Leptolepidites*, *Lycopodiacidites*, *Kraeuselisporites*, *Triancoraesporites*, *Uvaesporites* *Aratrisporites*, *Neoraistrickia*, *Acanthotriletes*, *Anapiculatisporites*, *Densoisporites*, *Limbosporites*, *Trizonites*		
Seed ferns	*Vitreisporites*, *Alisporites*		

Note: This summary is based upon comprehensive results of the *in situ* spore studies of the Mesozoic plants and their ecology based on Couper (1957); Harris (1961, 1964, 1969, 1979), Pocock & Jansonius (1969), van Konijnenburg-van Cittert (1971, 1978, 1993, 2002), Litwin (1985), Osborn & Taylor (1993), Balme (1995), Wang & Mei (1999), Deng & Chen (2001), Abbink, van Konijnenburg-van Cittert & Visscher (2004), Wang, Mosbrugger & Zhang (2005), Jiang *et al*. (2008), Guignard *et al*. (2009), Wang & Zhang (2010) and Wang *et al*. (2015).

4.c. *Cyathidites minor – Monosulcites fusiformis – Classopollis minor – Quadraeculina anellaeformis* (CMCQ) assemblage (samples HC24–HC32)

The assemblage CMCQ occurs in Members IV–VI of the Xujiahe Formation (Fig. 6) and is characterized by a significant dominance of gymnosperm pollen grains (relative abundance 64 %). Monosulcate pollen (*Monosulcites*, *Cycadopites* and *Chasmatosporites*) are the most prominent type. In comparison with the other two assemblages, a higher portion is represented by pollen attributed to seed ferns (8 %). The relatively high abundance of *Classopollis* (6 %) is also significant, a taxon that is virtually absent from the other two assemblages. Spores make up 36 % with a significant dominance of *Cyathidites* (10 %). Monolete spores are rare, comprising <1 % (Fig. 6).

5. Development of the vegetation

Based on the botanical affinity of the dispersed spore and pollen genera recovered from the studied successions within the Hechuan region of the Sichuan Basin (Table 1), a picture of a diverse Late Triassic ecosystem emerges. Although the vegetation is chiefly dominated by ferns and conifers, other plant groups are present in lower relative abundance. These include mosses, horsetails and lycopsids which vary considerably in relative abundance through the studied succession (Fig. 7). The overall evolution of the Late Triassic vegetation in the Hechuan region is suggested to have undergone changes from lowland fern forest to a mixed forest with more canopy trees.

The earliest Late Triassic DCKA ecosystem (represented in Member I and the base of Member III) was dominated by ferns, mainly Dipteridaceae/Matoniaceae together with a variety of other fern families including Cyatheaceae/Dicksoniaceae, Osmundaceae and Marattiaceae. These ferns, together with typical Triassic lycopsids and rare mosses, comprised the ground cover vegetation during the earliest part of Late Triassic time. The mid-storey was represented by gymnosperms related to cycads/bennettites/ginkgophytes. Canopy trees were

https://doi.org/10.1017/S0016756817000735 Published online by Cambridge University Press

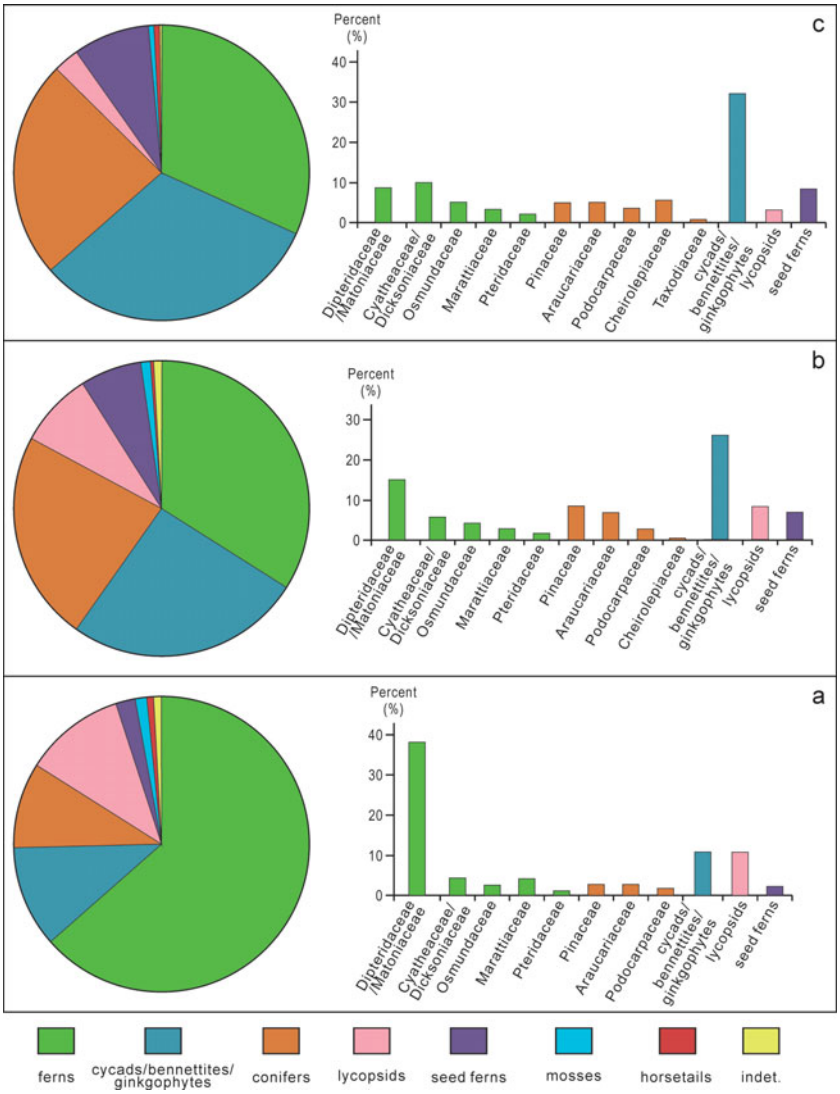

Figure 7. Palaeovegetation composition of the Xujiahe Formation from the Hechuan region. (a) DCKA assemblage (Member I and base of Member III); (b) CPDA assemblage (Member III); and (c) CMCQ assemblage (Members IV, V, VI).

relatively scarce, represented by Pinaceae, Araucariaceae and Podocarpaceae, and the pollen may have been transported in from elevated areas into the lowlands. Seed ferns existed, but made up a very limited portion of this ecosystem.

The CPDA ecosystem was characterized by dominance in gymnosperms, mainly represented by cycads/bennettites/ginkgophytes making up the mid-storey bush vegetation together with seed ferns. Canopy vegetation was represented by relatives of Pinaceae. The ferns are much less prominent in the CPDA assemblage compared to the older DCKA assemblage (Fig. 7b), and these were mainly represented by Dipteridaceae/Matoniaceae. Lycopsids are not as abundant compared with the DCKA assemblage. A new element, the family Cheirolepidiaceae (*Classopollis*), a group that was common during Jurassic and Early Cretaceous time around the world (Alvin, 1982; Vajda, 2001; Vajda & Wigforss-Lange, 2006; Jansson *et al.* 2008), interestingly appears in this assemblage.

In assemblage CMCQ, represented within the upper part of the Xujiahe Formation (Member V and VI), cycads/bennettites/ginkgophytes and conifers characterize the flora. It is interesting to note that Cyatheaceae/Dicksoniaceae show a sharp increase in abundance (average 10 %). Other fern families include Dipteridaceae/Matoniaceae, Osmundaceae, Marattiaceae and Pteridaceae. The mid-storey vegetation was dominated by monosulcate pollen producers, cycads/bennettites/ginkgophytes (Fig. 7c). Conifers including Cheirolepidiaceae, Araucariaceae, Pinaceae, Podocarpaceae and Taxodiaceae were prominent (average 24 %), making up the canopy. It is notable that Cheirolepidiaceae shows a remarkable increase in relative abundance and becomes common during this period (average 6 %). Seed ferns show an increasing trend (8 %). Lycopsids are less frequent, and mosses and horsetails are rare.

6. Palaeoclimatic interpretations

As a complement to the vegetation reconstruction based on the abundance data of pollen and spores related to their affinities, we have carried out

https://doi.org/10.1017/S0016756817000735 Published online by Cambridge University Press

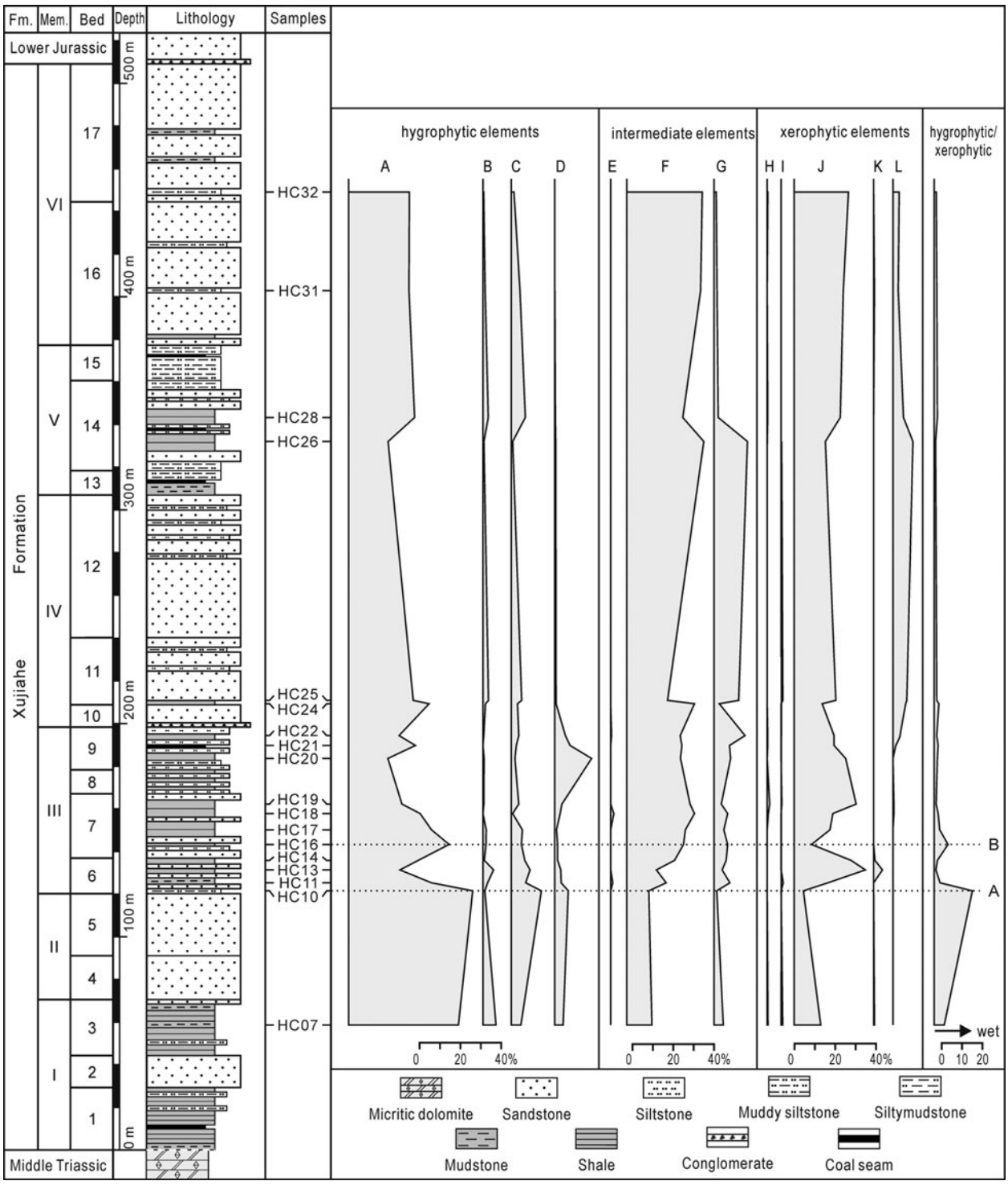

Figure 8. Relative abundances of the Spore-pollen Morphological Groups (SMGs) of the Xujiahe Formation from the Hechuan region. A, Trilete acavate laevigate or apiculate spores; B, Trilete acavate reticulate or murornate spores; C, Trilete cingulate or zonate spores; D, Monolete spores; E, *Ovalipollis* + *Perinopollenites*; F, Monosulcate pollen; G, Asaccate pollen; H, Monosaccate pollen; I, Trilete (proto) bisaccate pollen; J, Alete bisaccate pollen; K, Taeniate (proto) bisaccate pollen; L, *Classopollis* spp. A–D are considered to be hygrophytic elements, E–G intermediate and H–L xerophytic elements.

palaeoclimatic interpretations by applying the Spore-pollen Morphological Group (SMG) method (Visscher & Van der Zwan, 1981) and the Sporomorph EcoGroup model (SEG) (Abbink, 1998; Abbink, van Konijnenburg-van Cittert & Visscher, 2004).

Twelve Spore-pollen Morphological Groups (SMGs) A–L were identified in this study (Fig. 8), reflecting different ecological adaptations, including hygrophytic (water-loving, groups A–D), xerophytic (dry-loving, groups H–L) and intermediate elements (groups E–G). We have applied the ratio of hygrophytic elements to xerophytic elements (hygrophytic/xerophytic) as an index of humidity variation. The results (Fig. 8) show that the

https://doi.org/10.1017/S0016756817000735 Published online by Cambridge University Press

hygrophytic/xerophytic ratio is high in the lowermost part of the Xujiahe Formation, particularly at the base of Member III (Fig. 8, line A), indicating a humid pulse of short duration and expressed in one sample within the Xujiahe Formation. This is in agreement with the results based on the vegetation composition in Assemblage DCKA. The hygrophytic/xerophytic ratio is markedly low for the rest of the succession (with the exception for sample HC16; Fig. 8, line B), suggesting a drying trend upwards, interrupted by a short humid pulse.

Using the Sporomorph EcoGroup model (SEG) (Abbink, 1998; Abbink, van Konijnenburg-van Cittert & Visscher, 2004), we classified the palynomorphs into three SEG groups, including: (1) Lowland SEG; (2) Upland SEG; and (3) River SEG (Table 1, Fig. 9). Elements attributed to the Lowland SEG show a marked dominance in the Xujiahe Formation, with a maximum of 81 % and a minimum of 46 %; the River SEG and Upland SEG are less abundant. The total for the Lowland SEG and River SEG is a minimum of 69 % (Fig. 9). This implies that the studied area during Late Triassic time was represented by a general lake-marsh environment set in a lowland ecosystem. However, variations in the ecosystem and the climate during Late Triassic time are reflected in the palynological assemblages of this study, revealing that the ecosystem was not constant throughout this period as previously suggested (Huang & Lu, 1992; Wang *et al*. 2008, 2010).

As indicated by the hygrophytic elements (groups A–D; Fig. 8), the highest abundance of the Lowland SEG is found in the lowermost sample of Member III (Fig. 9, line A), corresponding to the highest values of the Lowland/Upland ratio and Lowland wet/dry ratio, the lowest value of the Upland SEG and a relatively high warm/cool ratio, suggesting a relatively warm and humid interval. The Lowland wet/dry ratio is only high in the lowermost two samples, and shows a striking upwards decreasing trend, suggesting a general drying trend. The Lowland SEG and the Lowland/Upland ratio show two smaller peaks at samples HC16 of Member III (Fig. 9, line B) and HC24 of Member IV (Fig. 9), indicating two short intervals of humid climate conditions. The Lowland warm/cool ratio shows an overall decreasing upwards trend in the Xujiahe Formation, but has a striking peak at sample HC25 of Member IV (Fig. 9, line C), indicating an overall cooling trend during the Late Triassic period interrupted by a short warmer climate interval.

Previous palynological and palaeobotanical studies from the Sichuan Basin have shown that the Late Triassic palaeoclimate was generally one of humid and warm tropics-subtropics (Huang & Lu, 1992; Wang *et al*. 2008, 2010). However, with our more detailed, high-resolution palynological study, a different picture emerges. Our data reveal a highly variable Late Triassic ecosystem represented by a warm and humid climate during the earliest Late Triassic period (Member I and base of Member III), followed by a cooler and drier interval interrupted by two wetter and one warmer episodes.

7. Discussion

Our palynological study indicates an overall cooling and drying trend during latest Norian–Rhaetian time, accompanied by a general decrease in ferns (mainly represented by trilete spores), an increase in gymnosperms (represented by bisaccate and monocolpate pollen), and a decline in diversity of both pollen and spores (Fig. 10). Similar results have been reported from coeval deposits in Xuanhan, northeastern Sichuan Basin, indicating a cooling and drying climate during the development of the uppermost part of the Xujiahe Formation (Li *et al*. 2016). The above outlined climate change is consistent with macrofloral studies of the Xujiahe Formation, which also implied a palaeoclimatic trend from humid to arid conditions (Huang & Lu, 1992). Palynological records from northwestern and central Europe, Western Australia and northeastern Greenland revealed a cooling during latest Triassic time (Hubbard & Boulter 1997, 2000) and the trend from humid to arid has also been noted from the Newark Basin (Kent & Olsen, 2000; Olsen & Kent, 2000) where it has been linked to the northwards drift of the North American continent. Palynological data from Austria and the United Kingdom indicated a warming trend from the Triassic to the Jurassic periods, interrupted by a cooler period (Bonis & Kürschner, 2012). Further, a bentho-planktonic study from the Austrian Alps suggested that cooling episodes might have occurred during latest Triassic time (Clémence *et al*. 2010). The above results may suggest a global cooling event during latest Triassic time. Tucker & Benton (1982) proposed climate-induced (increasing aridity) floral changes as a factor in Late Triassic tetrapod extinction. The present palynological record seems more consistent with a gradual ecosystem degradation extended over the Norian–Rhaetian interval. The cooling and drying climate from latest Norian to Rhaetian time may have caused a gradual ecosystem breakdown during latest Triassic time, and later triggered the end-Triassic biotic crisis.

8. Conclusions

Our detailed palynological investigation of Upper Triassic terrestrial deposits within the Sichuan Basin has revealed a well-preserved and diverse palynoflora.

(1) Our study reveals an ecosystem in change where a fern-dominated vegetation was replaced by conifers and cycadoids, supplemented by relative high portions of *Classopollis* in the uppermost Triassic strata. Palynological diversity patterns show a decreasing trend upsection.

(2) Three palynological assemblages were distinguished by variations in the abundance of major plant groups, reflecting remarkable changes in the

https://doi.org/10.1017/S0016756817000735 Published online by Cambridge University Press

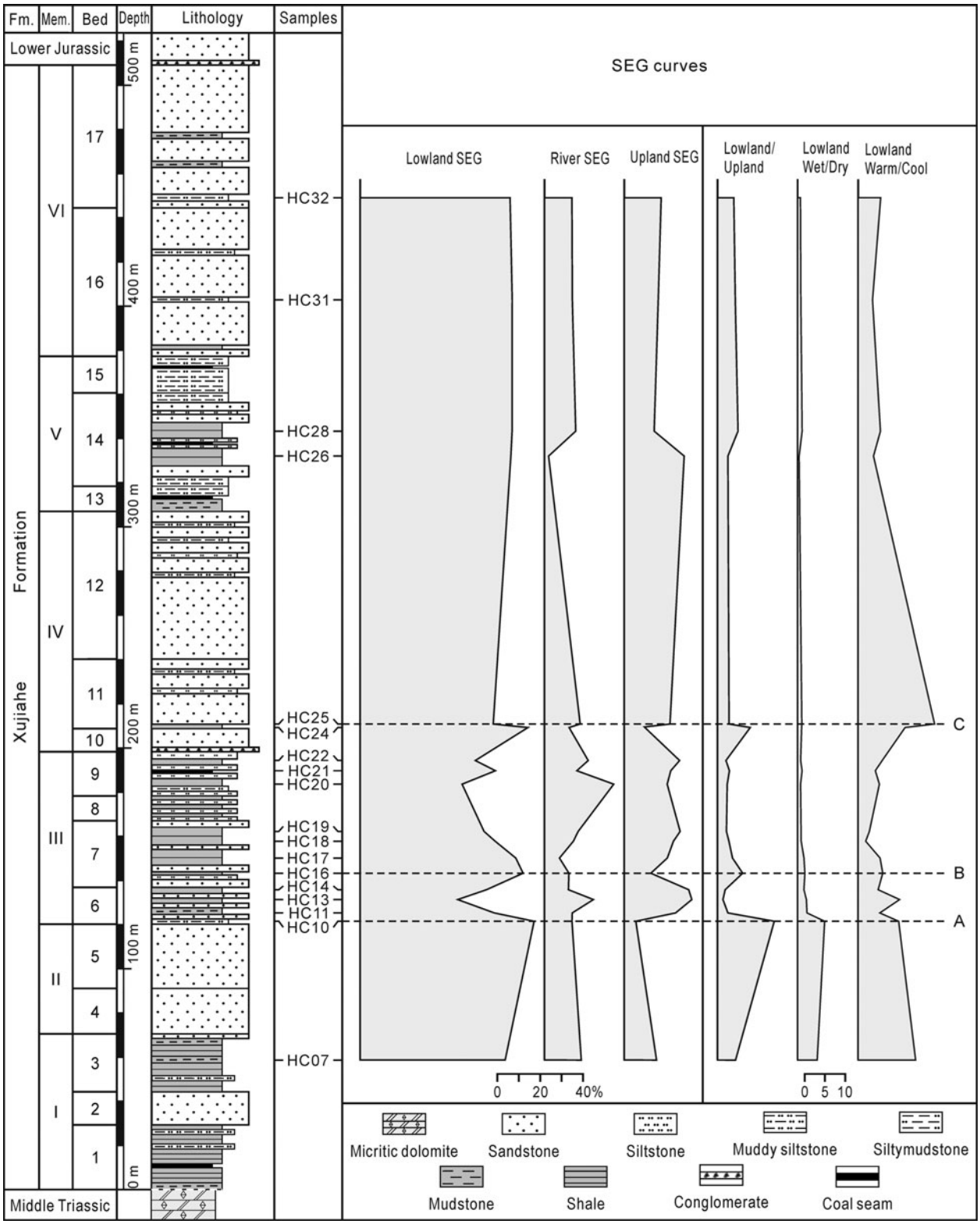

Figure 9. Relative abundances of the Sporomorph EcoGroups (SEGs) of the Xujiahe Formation from the Hechuan region.

terrestrial vegetation throughout the entire interval. Cycads/bennettites/ginkgophytes and conifers show an increasing trend into younger deposits, while ferns and lycopsids decrease in relative abundance.

(3) By applying the SMG method and SEG model analysis, we show that the early stage of the Late Triassic period was characterized by a relatively warm and humid climate which was followed by a cooler and drier interval. This demonstrates that the climate was not static, but rather variable.

(4) Our results reveal vegetation changes within the Sichuan Basin during the Late Triassic Period, adding to knowledge on biotic changes immediately prior to the end-Triassic event.

https://doi.org/10.1017/S0016756817000735 Published online by Cambridge University Press

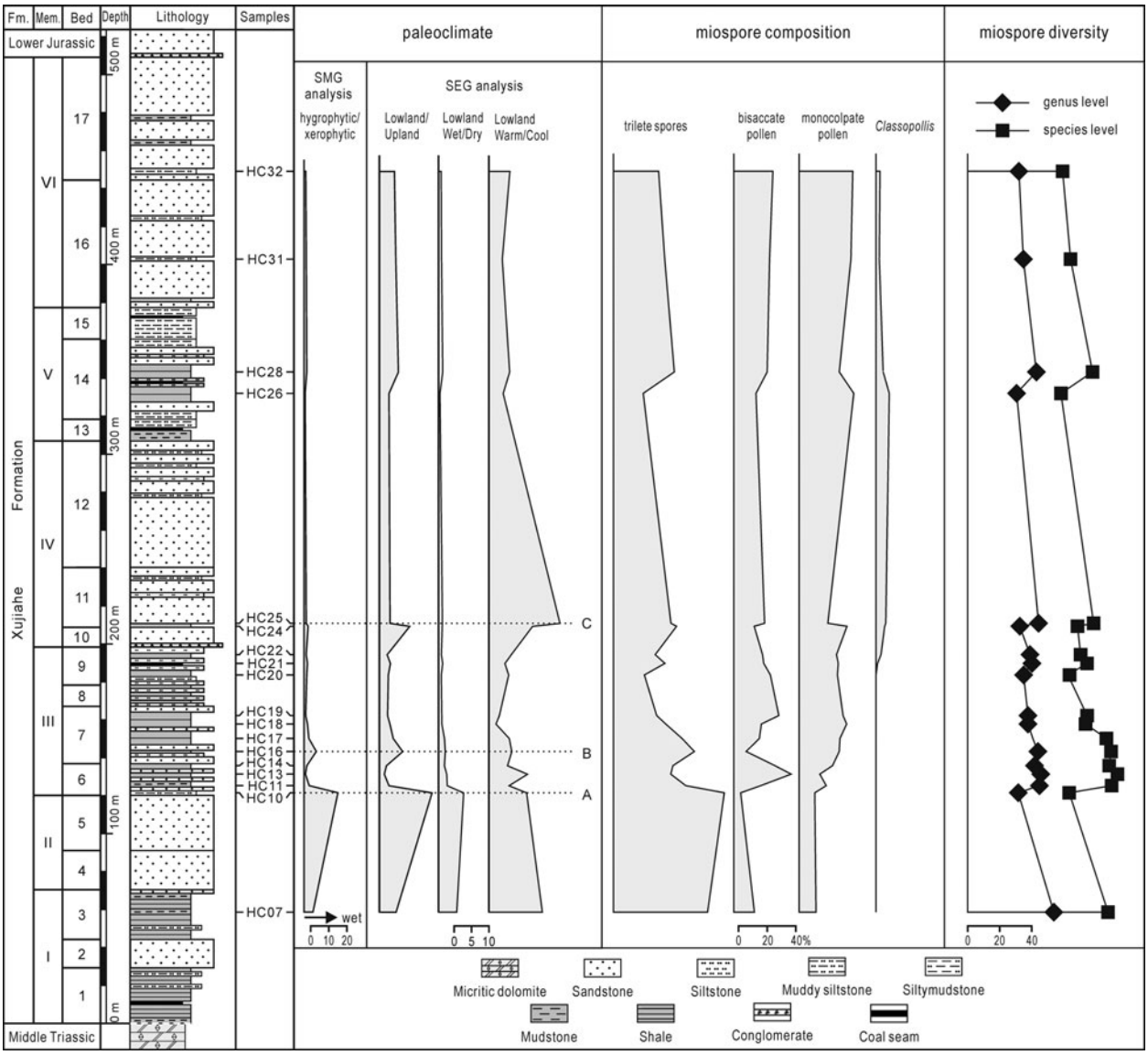

Figure 10. Palaeoclimate, miospore composition and miospore diversity of the Xujiahe Formation from the Hechuan region.

Acknowledgements. We acknowledge Xiaoping Xie, Ning Tian, Ning Zhou, Shucheng Xie, Mingsong Li and Ms Feng Limei for field and laboratory assistance. This work was financially supported by the Strategic Priority Research Program (B) of the Chinese Academy of Sciences (XDB18000000, XDPB0506); the National Natural Sciences Foundation of China (NSFC 41572014, 41688103); the State Key Program of Research and Development of Ministry of Science and Technology, China (2016YFC0600406); the State Key Laboratory of Palaeobiology and Stratigraphy (20172103); the Swedish Research Council (VR 2015–04264) and the Lund University Carbon Cycle Centre (LUCCI). This is a contribution to the IGCP project 632, sponsored by Unesco/IUGS. We also thank Evelyn Kustatscher and an anonymous reviewer for their constructive comments which led to the improvement of the manuscript.

Supplementary material

To view supplementary material for this article, please visit https://doi.org/10.1017/S0016756817000735.

References

Abbink, O. A. 1998. *Palynological investigations in the Jurassic of the North Sea region*. Ph.D. thesis, University of Utrecht, Utrecht, 191 pp. Published thesis.

Abbink, O. A., van, Konijnenburg-van Cittert, J. H. A. & Visscher, H. 2004. A sporomorph ecogroup model for the Northwest European Jurassic – Lower Cretaceous i: concepts and framework. *Netherlands Journal of Geosciences/Geologie en Mijnbouw* **83**(1), 17–38.

Akikuni, K., Hori, R., Vajda, V., Grant Mackie, J. & Ikehara, M. 2010. Stratigraphy of Triassic–Jurassic boundary sequences from the Kawhia coast and Awakino gorge, Murihiku Terrane, New Zealand. *Stratigraphy* **7**, 7–24.

Alvin, K. L. 1982. Cheirolepidiaceae: biology, structure and paleoecology. *Review of Palaeobotany and Palynology* **37**(1–2), 71–98.

Bachan, A. & Payne, J. 2016. Modelling the impact of pulsed CAMP volcanism on pCO_2 and $\delta^{13}C$ across the Triassic–Jurassic transition. *Geological Magazine* **153**(2), 252–70.

Bai, Y. H., Lu, M. N., Chen, L. Y. & Long, R. H. 1983. Mesozoic spore-pollen. In *Palaeontological Atlas of Southwest China, Microfossils* (ed. Chengdu Institute of Geology and Mineral Resources), pp. 520–653. Beijing: Geological Publishing House (in Chinese).

Balme, B. E. 1995. Fossil in situ spores and pollen grains: an annotated catalogue. *Review of Palaeobotany and Palynology* **87**(2–4), 81–323.

Bambach, R. K. 2006. Phanerozoic biodiversity mass extinctions. *Annual Review of Earth and Planetary Science* **34**, 127–55.

Benton, M. J. 1986. More than one event in the late Triassic mass extinction. *Nature* **321**, 857–61.

Benton, M. J. 1991. What really happened in the late Triassic? *Historical Biology* **5**(2–4), 263–78.

Bonis, N. R. & Kürschner, W. M. 2012. Vegetation history, diversity patterns, and climate change across the Triassic/Jurassic boundary. *Paleobiology* **38**(2), 240–64.

Bonis, N. R., Ruhl, M. & Kürschner, W. M. 2010. Milankovitch-scale palynological turnover across the Triassic–Jurassic transition at St. Audrie's Bay, SW UK. *Journal of the Geological Society* **167**(5), 877–88.

Callegaro, S., Baker, D. R., De Min, A., Marzoli, A., Geraki, K., Bertrand, H., Viti, C. & Nestola, F. 2014. Microanalyses link sulfur from large igneous provinces and Mesozoic mass extinctions. *Geology* **42**(10), 895–98.

Cao, J. Y. & Huang, X. M. 1980. Late Triassic and Early Jurassic spore-pollen assemblages from northeastern Sichuan. *Coal Geology and Exploration* **5**, 17–22 (in Chinese).

Clémence, M.-E., Gardin, S., Bartolini, A., Paris, G., Beaumont, V. & Guex, J. 2010. Bentho-planktonic evidence from the Austrian Alps for a decline in sea-surface carbonate production at the end of the Triassic. *Swiss Journal of Geosciences* **103**(2), 293–315.

Colbert, E. H. 1958. Tetrapod extinctions at the end of the Triassic Period. *Proceedings of the National Academy of Sciences of the USA* **44**(9), 973–77.

Couper, R. A. 1957. British Mesozoic microspores and pollen grains. A systematic and stratigraphic study. *Palaeontographica Abteilung B* **103**, 75–179.

Deng, S. H. & Chen, F. 2001. *The Early Cretaceous Filicopsida from northeast China*. Beijing: Geological Publishing House, 249 pp. (in Chinese with English summary).

Deng, S. H., Lu, Y. Z., Fan, R., Pan, Y. H., Cheng, X. S., Fu, G. B., Wang, Q. F., Pan, H. Z., Shen, Y. B., Wang, Y. Q., Zhang, H. C., Jia, C. K., Duan, W. Z. & Fang, L. H. 2010. *The Jurassic System of Northern Xinjiang, China*. Hefei: University of Science and Technology of China Press, 279 pp. (in Chinese and English).

Fu, G., Zhang, L. H., Yuan, Z. H. & Chen, B. 2010. Sedimentary environment research for Xujiahe Formation of the Upper Triassic series in Sichuan Basin. *Journal of Chongqing University of Science and Technology (Natural Sciences Edition)* **12**, 17–21 (in Chinese with English abstract).

Götz, A. E., Ruckwied, K., Pálfy, J. & Haas, J. 2009. Palynological evidence of synchronous changes within the terrestrial and marine realm at the Triassic/Jurassic boundary (Csővár section, Hungary). *Review of Palaeobotany and Palynology* **156**(3–4), 401–9.

Greene, S. E., Martindale, R. C., Ritterbush, K. A., Bottjer, D. J., Corsetti, F. A. & Berelson, W. M. 2012. Recognising ocean acidification in deep time: An evaluation of the evidence for acidification across the Triassic–Jurassic boundary. *Earth-Science Review* **113**(1–2), 72–93.

Guignard, G., Wang, Y. D., Ni, Q., Tian, N. & Jiang, Z. K. 2009. A dipteridaceous fern with in situ spores from the Lower Jurassic in Hubei, China. *Review of Palaeobotany and Palynology* **156**(1–2), 104–15.

Guy-Ohlson, D. 1981. Rhaeto-Liassic Palynostratigraphy of the Valhall Bore No. 1, Scania. *Geologiska Föreningens i Stockholm Förhandlingar* **103**(2), 233–48.

Hallam, A. 1990. The end-Triassic mass extinction event. In *Global Catastrophes in Earth History* (eds V. L. Sharpton & P. D. Ward), pp. 577–83. Geological Society of America, Special Paper no. 247.

Hallam, A. 2002. How catastrophic was the end-Triassic mass extinction? *Lethaia* **35**(2), 147–57.

Harris, T. M. 1961. *The Yorkshire Jurassic flora, I. Thallophyta - Pteridophyta*. London: British Museum (Natural History), London, 212 pp.

Harris, T. M. 1964. *The Yorkshire Jurassic flora, II. Caytoniales, Cycadales and Pteridosperms*. London: British Museum (Natural History), London, 191 pp.

Harris, T. M. 1969. *The Yorkshire Jurassic flora, III. Bennettitales*. London: British Museum (Natural History), London, 186 pp.

Harris, T. M. 1979. *The Yorkshire Jurassic flora, V. Coniferales*. London: British Museum (Natural History), London, 166 pp.

Hesselbo, S. P., McRoberts, C. A. & Pálfy, J. 2007. Triassic–Jurassic boundary events: Problems, progress, possibilities. *Palaeogeography, Palaeoclimatology, Palaeoecology* **244**, 1–10.

Hesselbo, S. P., Robinson, S. A., Surlyk, F. & Piasecki, S. 2002. Terrestrial and marine extinction at the Triassic–Jurassic boundary synchronized with major carbon-cycle perturbation: a link to initiation of massive volcanism? *Geology* **30**(3), 252–4.

Hönisch, B., Ridgwell, A., Schmidt, D. N., Thomas, E., Gibbs, S. J., Sluijs, A., Zeebe, R., Kump, L., Martindale, R. C., Greene, S. E., Kiessling, W., Ries, J., Zachos, J. C., Royer, D. L., Barker, S., Marchitto, T. M., Moyer, R., Pelejero, C., Ziveri, P., Foster, G. L. & Williams, B. 2012. The geological record of ocean acidification. *Science* **335**, 1058–63.

Huang, Q. S. 1995. Paleoclimate and coal-forming characteristics of the Late Triassic Xujiahe stage in northern Sichuan. *Geological Review* **41**(1), 92–9 (in Chinese with English abstract).

Huang, Q. S. & Lu, S. M. 1992. The primary studies on the palaeoecology of the Late Triassic Xujiahe flora in eastern Sichuan. *Earth Science-Journal of China University of Geosciences* **17**(3), 329–35 (in Chinese with English abstract).

Huang, X. P. 1991. The spore-pollen assemblage from the Xujiahe Formation of Huayingshan area, northern Sichuan. *Coal Geological Exploration of Sichuan* **9**, 28–33 (in Chinese).

Hubbard, R. N. L. B. & Boulter, M. C. 1997. Mid Mesozoic floras and climates. *Palaeontology* **40**, 43–70.

Hubbard, R. N. L. B. & Boulter, M. C. 2000. Phytogeography and paleoecology in western Europe and eastern Greenland near the Triassic–Jurassic boundary. *Palaios* **15**(2), 120–131.

Ikeda, M., Hori, R. S., Okada, Y. & Nakada, R. 2015. Volcanism and deep-ocean acidification across the end-Triassic extinction event. *Palaeogeography, Palaeoclimatology, Palaeoecology* **440**, 725–33.

Jansson, I.-M., McLoughlin, S., Vajda, V. & Pole, M., 2008. An Early Jurassic flora from the Clarence-Moreton Basin, Australia. *Review of Palaeobotany and Palynology* **150**, 5–21.

Jiang, D. X., Wang, Y. D., Robbins, E. I., Wei, J. & Tian, N. 2008. Mesozoic non-marine petroleum source rocks determined by palynomorphs in the Tarim Basin, Xinjiang, northwestern China. *Geological Magazine* **145**(6), 868–85.

Kent, D. V. & Olsen, P. E. 2000. Magnetic polarity stratigraphy and paleolatitude of the Triassic-Jurassic Blomidon Formation in the Fundy Basin (Canada): implications for early Mesozoic tropical climate gradients. *Earth Planetary Science Letters* **179**(2), 311–24.

Larsson, L. M. 2009. Palynostratigraphy of the Triassic–Jurassic transition in southern Sweden. *GFF* **131**(1–2), 147–63.

Lathuilière, B. & Marchal, D. 2009. Extinction, survival and recovery of corals from the Triassic to Middle Jurassic times. *Terra Nova* **21**, 57–66.

Li, L. Q. & Wang, Y. D. 2016. Late Triassic palynofloras in the Sichuan Basin, South China: Synthesis synthesis and perspective. *Palaeoworld* **25**(2), 212–38.

Li, L. Q., Wang, Y. D., Liu, Z. S., Zhou, N. & Wang, Y. 2016. Late Triassic palaeoclimate and palaeoecosystem variations inferred by palynological record in the northeastern Sichuan Basin, China. *Paläontologische Zeitschrift* **90**(2), 327–48.

Li, M. S., Zhang, Y., Huang, C. J., Ogg, J., Hinnov, L., Wang, Y. D., Zou, Z. Y. & Li, L. Q. 2017. Astronomical tuning and magnetostratigraphy of the Upper Triassic Xujiahe Formation of South China and Newark Supergroup of North America: implications for the Late Triassic time scale. *Earth and Planetary Science Letters* **475**, 207–223.

Li, W. B. 1974. Triassic pollen and spores. In *Handbook of Stratigraphy and Palaeontology of Southwest China* (ed. Nanjing Institute of Geology and Palaeontology, Academia Sinica).), pp. 362–70. Beijing: Science Press (in Chinese).

Lindström, S. 2016. Palynofloral patterns of terrestrial ecosystem change during the end-Triassic event – a review. *Geological Magazine* **153**(2), 223–51.

Litwin, R. J. 1985. Fertile organs and in situ spores of ferns from the Late Triassic Chinle Formation of Arizona and New Mexico, with discussion of the associated dispersed spores. *Review of Palaeobotany and Palynology* **44**(1–2), 101–46.

Liu, Z. S. 1982. Mesozoic spore-pollen assemblages from Hechuan, Zitong and Bazhong counties, Sichuan Province. In *Continental Mesozoic Stratigraphy and Paleontology in Sichuan Basin of China* (ed. Writing Group of Continental Mesozoic Stratigraphy and Paleontology in Sichuan Basin), pp. 440–61. Chengdu: People's Publishing House of Sichuan (in Chinese).

Liu, Z. S., Li, L. Q. & Wang, Y. D. 2015a. Late Triassic spore-pollen assemblage from Xuanhan of Sichuan, China. *Acta Micropalaeontologica Sinica* **32**(1), 43–62 (in Chinese with English abstract).

Liu, Z. S., Li, L. Q. & Wang, Y. D. 2015b. Late Triassic spore-pollen assemblage of the Xujiahe Formation from Hechuan of Chongqing, China. *Acta Palaeontologica Sinica* **54**(3), 279–304 (in Chinese with English abstract).

Lu, M. N. & Wang, R. S. 1987. Late Triassic–Early Jurassic spore-pollen assemblages in Sichuan Basin and their distribution. In *Professional Papers of Petroleum Stratigraphy and Palaeontology* (ed. Editorial Committee of Professional Papers of Petroleum Stratigraphy and Palaeontology), pp. 207–12. Beijing: Geological Publishing House (in Chinese).

Lucas, S. G. & Tanner, L. H. 2007. The non-marine Triassic–Jurassic boundary in the Newark Supergroup of eastern North America. *Earth-Science Reviews* **84**(1–2), 1–20.

Lucas, S. G. & Tanner, L. H. 2008. Reexamination of the end-Triassic mass extinction. In *Mass Extinction* (ed. A. M. T. Elewa), pp. 65–102. Berlin, Heidelberg: Springer, 252 pp.

Lucas, S. G. & Tanner, L. H. 2015. End-Triassic non-marine biotic events. *Journal of Palaeogeography* **4**(4), 331–48.

Lund, J. J. 1977. Rhaetic to Lower Liassic palynology of the onshore south-eastern North Sea Basin. *Danmarks Geologiske Undersøgelse* **109**(2), 1–103.

Mander, L., Kürschner, W. M. & McElwain, J. C. 2013. Palynostratigraphy and vegetation history of the Triassic–Jurassic transition in East Greenland. *Journal of the Geological Society* **170**(1), 37–46.

Marzoli, A., Bertrand, H., Knight, K. B., Cirilli, S., Buratti, N., Vérati, C., Nomade, S., Renne, P. R., Youbi, N., Martini, R., Allenbach, K., Neuwerth, R., Rapaille, C., Zaninetti, L. & Bellieni, G. 2004. Synchrony of the Central Atlantic Magmatic Province and the Triassic–Jurassic boundary climatic and biotic crisis. *Geology* **32**(11), 973–76.

Marzoli, A., Renne, P. R., Piccirillo, E. M., Ernesto, M., Bellieni, G. & De Min, A. 1999. Extensive 200-million-year-old continental flood basalts of the Central Atlantic magmatic province. *Science* **284**, 616–18.

McElwain, J. C., Beerling, D. J. & Woodward, F. I. 1999. Fossil plants and global warming at the Triassic–Jurassic boundary. *Science* **285**, 1386–90.

McElwain, J. C., Popa, M. E., Hesselbo, S. P., Haworth, M. & Surlyk, F. 2007. Macroecological responses of terrestrial vegetation to climatic and atmospheric change across the Triassic/Jurassic boundary in East Greenland. *Paleobiology* **33**(4), 547–73.

McElwain, J. C., Wagner, P. J. & Hesselbo, S. P. 2009. Fossil plant relative abundances indicate sudden loss of Late Triassic biodiversity in East Greenland. *Science* **324**, 1554–6.

Milner, A. 1989. Late extinctions of amphibians. *Nature* **338**, 117.

Olsen, P. E. & Kent, D. V. 2000. High resolution early Mesozoic Pangean climatic transect in lacustrine environments. In *Epicontinental Triassic, Volume 3* (eds G. Bachmann & I. Lerche), pp. 1475–96. E. Schweizerbart'sche Verlagsbuchhandlung, Stuttgart, Zentralblatt fur Geologie und Palaontologie, VIII.

Olsen, P. E., Kent, D. V., Sues, H. -D., Koeberl, C., Huber, H., Montanari, A., Rainforth, E. C., Fowell, S. J., Szajna, M. J. & Hartline, B. W. 2002. Ascent of dinosaurs linked to an iridium anomaly at the Triassic–Jurassic boundary. *Science* **296**, 1305–7.

Olsen, P. E., Shubin, N. H. & Anders, M. H. 1987. New Early Jurassic tetrapod assemblage constrain Triassic–Jurassic tetrapod extinction event. *Science* **237**, 1025–9.

Osborn, J. M. & Taylor, T. N. 1993. Pollen morphology and ultrastructure of the corystospermales - permineralized in-situ grains from the Triassic of Antarctica. *Review of Palaeobotany and Palynology* **79**(3–4), 205–19.

Pálfy, J., Mortensen, J. K., Carter, E. S., Smith, P. L., Friedman, R. M. & Tipper, H. W. 2000. Timing the end-Triassic mass extinction: First on land, then in the sea? *Geology* **28**(1), 39–42.

Pedersen, K. R. & Lund, J. J. 1980. Palynology of the plant-bearing Rhaetian to Hettangian Kap Stewart Formation,

Scoresby Sund, East Greenland. *Review of Palaeobotany and Palynology* **31**, 1–69.

Pieńkowski, G., Niedźwiedzki, G. & Waksmundzka, M. 2012. Sedimentological, palynological and geochemical studies of the terrestrial Triassic–Jurassic boundary in northwestern Poland. *Geological Magazine* **149**(2), 308–32.

Pocock, S. A. J. & Jansonius, J. 1969. Redescription of some fossil gymnospermous pollen (*Chasmatosporites*, *Marsupipollenites*, *Ovalipollis*). *Canadian Journal of Botany* **47**, 155–65.

Pott, C. & McLoughlin, S. 2009. Bennettitalean foliage in the Rhaetian–Bajocian (latest Triassic–Middle Jurassic) floras of Scania, southern Sweden. *Review of Palaeobotany and Palynology* **158**(1–2), 117–66.

Pott, C. & McLoughlin, S. 2011. The Rhaetian Flora of Rögla, Northern Scania, Sweden. *Palaeontology* **54**(5), 1025–51.

Raup, D. M. & Sepkoski, Jr. J. J. 1982. Mass extinctions in the marine fossil record. *Science* **215**, 1501–3.

Richoz, S., van de Schootbrugge, B., Pross, J., Püttmann, W., Quan, T. M., Lindström, S., Heunisch, C., Fiebig, J., Maquil, R., Schouten, S., Hauzenberger, C. A. & Wignall, P. B. 2012. Hydrogen sulphide poisoning of shallow seas following the end-Triassic extinction. *Nature Geoscience* **5**, 662–7.

Ruckwied, K. & Götz, A. E. 2009. Climate change at the Triassic/Jurassic boundary: palynological evidence from the Furkaska section (Tatra Mountains, Slovakia). *Geologica Carpathica* **60**(2), 139–49.

Ruckwied, K., Götz, A. E., Pálfy, J. & Torok, A. 2008. Palynology of a terrestrial coal-bearing series across the Triassic/Jurassic boundary (Mecsek Mts, Hungary). *Central European Geology* **51**(1), 1–15.

Ruhl, M., Bonis, N. R., Reichart, G.-J., Damsté, J. S. S. & Küerschner, W. F. 2011. Atmospheric carbon injection linked to end-Triassic mass extinction. *Science* **333**, 430–4.

Schaller, M. F., Wright, J. D. & Kent, D. V. 2011. Atmospheric pCO_2 perturbations associated with the Central Atlantic magmatic province. *Science* **331**, 1404–9.

Schaller, M. F., Wright, J. D., Kent, D. V. & Olsen, P. E. 2012. Rapid emplacement of the Central Atlantic Magmatic Province as a net sink for CO_2. *Earth and Planetary Science Letters* **323**, 27–39.

Schoene, B., Guex, J., Bartolini, A., Schaltegger, U. & Blackburn, T. J. 2010. Correlating the end-Triassic mass extinction and flood basalt volcanism at the 100 ka level. *Geology* **38**, 387–90.

Sepkoski, Jr. J. J. 1996. Patterns of Phanerozoic extinction: a perspective from global databases. In *Global Events and Event Stratigraphy* (ed. O. H. Walliser), pp. 35–51. New York: Springer-Verlag.

Sha, J. G., Olsen, P. E., Pan, Y. H., Xu, D. Y., Wang, Y. Q., Zhang, X. L., Yao, X. G. & Vajda, V. 2015. Triassic–Jurassic climate in continental high-latitude Asia was dominated by obliquity-paced variations (Junggar Basin, Ürümqi, China). *Proceedings of the National Academy of Sciences of the United States of America* **112**(12), 3624–9.

Sha, J. G., Vajda, V., Pan, Y. H., Larsson, L., Yao, X. G., Zhang, X. L., Wang, Y. Q., Cheng, X. S., Jiang, B. Y., Deng, S. H., Chen, S. W. & Peng, B. 2011. Stratigraphy of the Triassic–Jurassic Boundary Successions of the Southern Margin of the Junggar Basin, Northwestern China. *Acta Geologica Sinica* **85**(2), 421–36.

Shang, Y. K. & Li, W. B. 1992. Triassic and Jurassic sporepollen assemblages from northwestern Sichuan. *Bulletin of Nanjing Institute of Geology and Palaeontology, Academia Sinica* **13**, 138–208 (in Chinese with English abstract).

Steinthorsdottir, M., Jeram, A. J. & McElwain, J. C. 2011. Extremely elevated CO_2 concentrations at the Triassic/Jurassic boundary. *Palaeogeography, Palaeoclimatology, Palaeoecology* **308**(3–4), 418–32.

Tanner, L. H., Lucas, S. G. & Chapman, M. G. 2004. Assessing the record and causes of Late Triassic extinctions. *Earth-Science Reviews* **65**, 103–39.

Tucker, M. E. & Benton, M. J. 1982. Triassic environments, climates and reptile evolution. *Palaeogeography, Palaeoclimatology, Palaeoecology* **40**, 361–79.

Vajda, V. 2001. Aalenian to Cenomanian palynofloras of SW Scania, Sweden. *Acta Paleontologica Polonica* **46**, 403–26.

Vajda, V. & Bercovici, A. 2014. The global vegetation pattern across the Cretaceous–Paleogene mass extinction interval: a template for other extinction events. *Global and Planetary Change* **122**, 29–49.

Vajda, V., Calner, M. & Ahlberg, A. 2013. Palynostratigraphy of dinosaur footprint-bearing deposits from the Triassic–Jurassic boundary interval of Sweden. *GFF* **135**(1), 120–30.

Vajda, V. & Wigforss-Lange, J. 2006. The Jurassic–Cretaceous transition of Southern Sweden – palynological and sedimentological interpretation. *Progress in Natural Science* **16**, 1–38.

van de Schootbrugge, B. & Wignall, P. B. 2016. A tale of two extinctions: converging end-Permian and end-Triassic scenarios. *Geological Magazine* **153**(2), 332–54.

van de Schootbrugge, B., Quan, T. M., Lindström, S., Püttmann, W., Heunisch, C., Pross, J., Fiebig, J., Petschick, R., Röhling, H. G., Richoz, S., Rosenthal, Y. & Falkowski, P. G. 2009. Floral changes across the Triassic/Jurassic boundary linked to flood basalt volcanism. *Nature Geoscience* **2**(8), 589–94.

van Konijnenburg-van Cittert, J. H. A. 1971. In situ gymnosperm pollen from the Middle Jurassic of Yorkshire. *Acta Botanica Neerlandica* **20**, 1–97.

van Konijnenburg-van Cittert, J. H. A. 1978. Osmundaceous spores in situ from the Jurassic of Yorkshire, England. *Review of Palaeobotany and Palynology* **26**, 125–41.

van Konijnenburg-van Cittert, J. H. A. 1993. A review of the Matoniaceae based on in situ spores. *Review of Palaeobotany and Palynology* **78**, 235–67.

van Konijnenburg-van Cittert, J. H. A. 2002. Ecology of some Late Triassic to Early Cretaceous ferns in Eurasia. *Review of Palaeobotany and Palynology* **119**, 113–24.

Visscher, H. & Van der Zwan, C. J. 1981. Palynology of the Circum-Mediterranean Triassic: Phytogeographical phytogeographical and palaeoclimatological implications. *Geologische Rundschau* **70**(2), 625–34.

Wang, Q. W., Kan, Z. Z., Liu, X. H., Liang, B. & Zhu, B. 2008. The Mesozoic sporopollen assemblage in the Sichuan Basin and its significance to paleovegetation and paleoclimate. *Acta Geologica Sichuan* **28**(2), 89–95 (in Chinese with English abstract).

Wang, Y. D., Fu, B. H., Xie, X. P., Huang, Q. S., Li, K., Li, G., Liu, Z. S., Yu, J. X., Pan, Y. H., Tian, N. & Jiang, Z. K. 2010. *The Terrestrial Triassic and Jurassic Systems in the Sichuan Basin, China*. Hefei: University

https://doi.org/10.1017/S0016756817000735 Published online by Cambridge University Press

of Science and Technology of China Press, 216 pp. (in Chinese and English).

Wang, Y. D., Li, L. Q., Guignard, G., Dilcher, D. L., Xie, X. P., Tian, N., Zhou, N. & Wang, Y. 2015. Fertile structures with in situ spores of a dipterid fern from the Triassic in southern China. *Journal of Plant Research* **128**(3), 445–57.

Wang, Y. D. & Mei, S. W. 1999. Fertile organs and in situ spores of a matoniaceous fern from the Lower Jurassic of West Hubei. *Chinese Science Bulletin* **44**(14), 1333–7.

Wang, Y. D., Mosbrugger, V. & Zhang, H. 2005. Early to Middle Jurassic vegetation and climatic events in the Qaidam Basin, Northwest China. *Palaeogeography, Palaeoclimatology, Palaeoecology* **224**(1–3), 200–16.

Wang, Y. D. & Zhang, H. 2010. Fertile organs and in situ spores of a new dipteridaceous fern (*Hausmannia sinensis*) from the Jurassic of northern China. *Proceedings of the Royal Society B-Biological Sciences* **277**, 311–20.

Whiteside, J. H., Olsen, P. E., Eglinton, T., Brookfield, M. E. & Sambrotto, R. N. 2010. Compound-specific carbon isotopes from Earth's largest flood basalt eruptions directly linked to the end-Triassic mass extinction. *Proceedings of the National Academy of Sciences of the United States of America* **107**, 6721–5.

Wignall, P. B. 2001. Large igneous provinces and mass extinctions. *Earth-Science Reviews* **53**, 1–33.

Wignall, P. B. & van de Schootbrugge, B. 2016. Middle Phanerozoic mass extinctions and a tribute to the work of Professor Tony Hallam. *Geological Magzine* **153**(2), 195–200.

Wotzlaw, J.-F., Guex, J., Bartolini, A., Gallet, Y., Krystyn, L., McRoberts, C. A., Taylor, D., Schoene, B. & Schaltegger, U. 2014. Towards accurate numerical calibration of the Late Triassic: High-precision U-Pb geochronology constraints on the duration of the Rhaetian. *Geology* **42**(7), 571–4.

Ye, M. N., Liu, X. Y., Huang, G. Q., Chen, L. X., Peng, S. J., Xu, A. F. & Zhang, B. X. 1986. *Late Triassic and Early–Middle Jurassic Fossil Plants from Northeastern Sichuan*. Hefei: Anhui Science and Technology Publishing House, 141 pp. (in Chinese with English summary).

Yuan, Y. C. 1989. The Late Triassic spore-pollen assemblage from the Libi Gorge, Beibei, Sichuan. *Coal Geological Exploration of Sichuan* **7**, 13–8 (in Chinese).

Zhang, L. J. 1984. *Late Triassic Spores and Pollen from Central Sichuan*. Paleontologia Sinica, New Series No. 8 (Whole no. 167). Beijing: Science Press, 100 pp. (in Chinese with English summary).